

OPTICAL FIBRES

PACS numbers: 42.81.Bm; 42.81.Dp; 42.81.Gs
DOI: 10.1070/QE2011v041n03ABEH014508

Highly birefringent low-mode-asymmetry microstructured optical fibres

A.N. Denisov, A.E. Levchenko, S.L. Semjonov, E.M. Dianov

Abstract. **A novel birefringent microstructured fibre (BMF) design is proposed, and its birefringence and dispersion characteristics are analysed using the finite element method. The results indicate that the proposed BMF design ensures high birefringence ($\sim 5\times10^{-3}$) at a low mode asymmetry. At a certain core ellipticity, the BMF configurations considered may have equal mode field sizes along two orthogonal axes.**

Keywords: *microstructured optical fibres, birefringence.*

1. Introduction

There has been unabated interest in the properties and potential applications of microstructured optical fibres since their advent [1, 2]. This is due to their unique characteristics, which differ markedly from those of conventional optical fibres [3–5]: wide single-mode range, unusual dispersion characteristics, increased birefringence and others.

Birefringent microstructured fibres (BMFs) of various designs were first reported in Refs [6–9]. Owing to their high birefringence, which varies little with temperature [10], BMFs are used for polarised supercontinuum generation [11–13], physical measurements [14–16], Bragg-grating [17, 18] and long-period grating inscription [19, 20] and other purposes, and are at present commercially available.

Labonte et al. [21] proposed a simple analytical model for evaluating the birefringence related to the core shape in BMFs that guide light through modified total internal reflection. They considered the three most widespread BMF designs: with two increased air holes near the core (proposed by Suzuki et al. [9]), with two defects in the form of missing holes (proposed by Hansen et al. [8]) and with three holes missing. The fibre core was represented by an equivalent rectangle [21], whose propagation constants were determined using an approximate analytical solution known for rectangular dielectric waveguides. In the case of the LP_{01} fundamental mode, the phase birefringence is given by [21]

$$B \approx \frac{\sqrt{n_1^2 - n_2^2}}{4\pi\bar{n}n_1^2}\left(\frac{\lambda}{b}\right)^3\left[1-\left(\frac{b}{a}\right)^3\right], \qquad (1)$$

A.N. Denisov, A.E. Levchenko, S.L. Semjonov, E.M. Dianov Fiber Optics Research Center, Russian Academy of Sciences, ul. Vavilova 38, 119333 Moscow, Russia; e-mail: denisov@fo.gpi.ru

Received 24 November 2010
Kvantovaya Elektronika **41** (3) 243–248 (2011)
Translated by O.M. Tsarev

where λ is the wavelength; n_1 and n_2 are the effective refractive indices of the fibre core and cladding, respectively; $\bar{n}$ is the average effective refractive index for two orthogonally polarised modes; and a and b are, respectively, the larger and smaller side lengths of the equivalent rectangle. Therefore, the birefringence of the BMFs considered by Labonte et al. [21] depends, in particular, on the relative difference between the core sizes along the two axes. Consequently, high birefringence can be reached by considerably increasing the a/b ratio, which would lead to a high azimuthal mode asymmetry in such fibres.

To quantify the mode asymmetry, we use a w parameter defined as the relative difference between the mode field sizes (full width at half intensity) along two orthogonal axes, that is, as the ratio of the difference between the mode field sizes to their average:

$$w = \frac{2(W_x - W_y)}{W_x + W_y}, \qquad (2)$$

where W_x and W_y are the mode field sizes along the two orthogonal axes. Typical w values for the mode field profiles calculated by Choi et al. [13] and Lee et al. [22] for BMFs are $\sim$0.45 and $\sim$0.36, respectively. At such w values, high power losses arise when BMFs are coupled to standard, circular-core fibres or when circular laser beams are used. To reduce such losses, Xiong and Wadsworth [12] used a BMF similar to those in Refs [9, 22] but with a reduced hole diameter ratio, $d_2/d_1 = 1.7$ (instead of $d_2/d_1 = 1.9$ in Ref. [22]). This reduced the core ellipticity to 1.25 and the measured coupling loss to 6% (the mode field profile was not reported by Xiong and Wadsworth [12], so w is unknown). At the same time, the 1.064-μm birefringence dropped to $\sim 1.24\times10^{-4}$.

The BMF design we propose here ensures high birefringence at a small mode asymmetry parameter, w.

2. Novel BMF geometry

The key features of the BMF design under consideration are that there is one or several concentric rings of holes of the same diameter around an elliptical or circular core and that the holes are the same distance apart except for one or two pairs of holes in the first ring, which are a greater distance apart.

One configuration of such BMFs is displayed in Fig. 1a. The BMF core (dashed line) is elliptical or circular in shape. The surrounding holes, of diameter d, are distance Λ apart (centre-to-centre distance), except for two holes, which are a greater distance, Λ_1, apart. Distance Λ from these two holes, there is another hole. The increased bridge (opening) between the holes has a width $Z = \Lambda_1 - d$. The diameters of the ellipti-

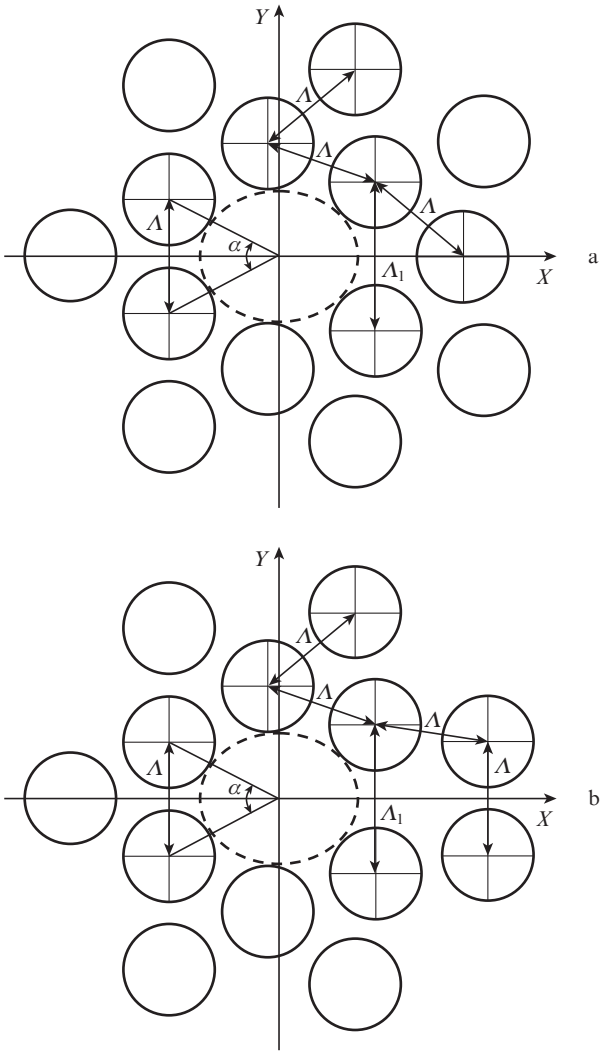

Figure 1. (a) 6117*ec* and (b) 6125*ec* structures: $d/\Lambda = 0.8$, $\Lambda_1/\Lambda = 1.3$, $e = 1.2$.

cal core along and across the opening are D_x and D_y, respectively. The BMF core ellipticity is $e = D_x/D_y$. Usually, ellipticity is defined as the minor to major axis ratio. Accordingly, $e \leqslant 1$. Since the structures under consideration have a special direction, that along the opening, it is more relevant to use the above definition. A BMF with $e > 1$ then has an elliptical core elongated along the opening. An elliptical core with $e < 1$ is elongated across the opening. The holes of the second ring 'close' the spaces between the holes of the first ring, and each of them is distance Λ from its two nearest holes in the first ring. If necessary, the number of rings can be increased. At large d/Λ ratios, however, two rings of holes ensure a sufficiently low leakage loss level, so we consider here single- and two-ring BMF designs.

For convenience, we use the following notation for BMF structures: *MNKLsf*, where M and N are, respectively, the numbers of holes and openings in the first ring; K is the number of intermediate holes that close openings; L is the number of holes in the second ring ($L = 0$ if there are no such holes); s specifies whether the core is elliptical (e) or circular (c); and f specifies whether the holes are circular (c) or elliptical (e). Accordingly, the BMF structure shown in Fig. 1a is denoted as 6117*ec*.

Figure 1b shows a 6125*ec* structure, which differs from the configuration displayed in Fig. 1a in that the opening between the holes of the first ring is closed by two holes, which increases the depth of the opening. These holes are distance Λ apart and are the same distance from the holes of the first ring. That the second ring comprises only five holes is the result of the relatively small difference between Λ_1 and Λ, so that the excess three holes do not reduce the leakage loss.

Another configuration of the proposed BMF design, with two increased openings, is displayed in Fig. 2. Figure 2a shows a 5227*ec* structure, with two identical openings, each closed by one hole. The 5243*ec* structure in Fig. 2b has two identical openings, each closed by two holes. BMFs may have openings that differ in width or are closed by different numbers of holes, but such configurations will not be considered in this study.

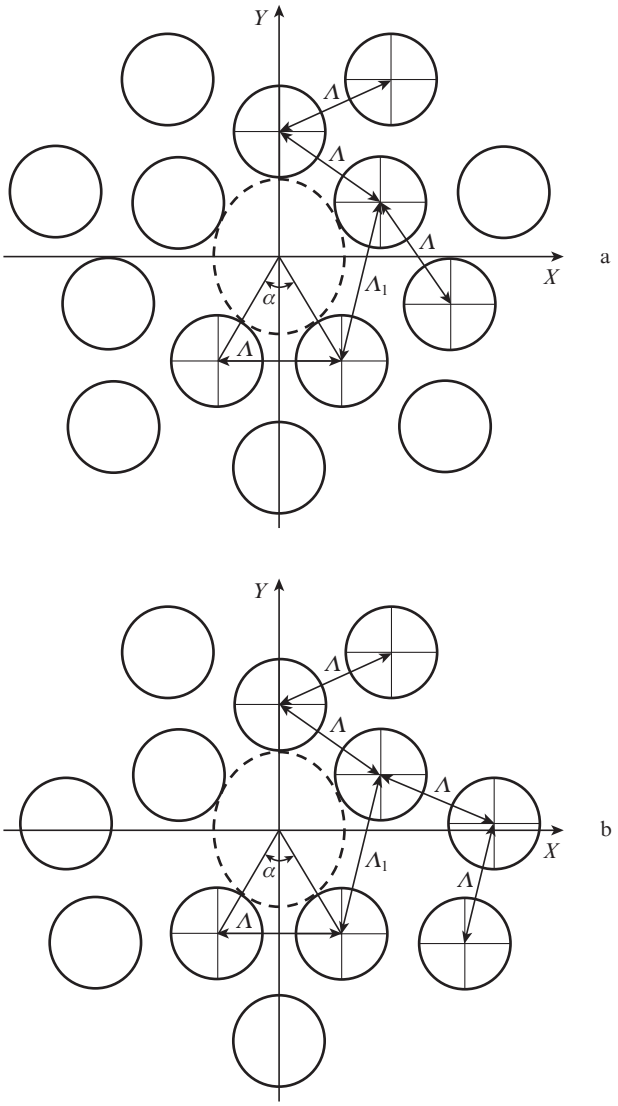

Figure 2. (a) 5227*ec* and (b) 5243*ec* structures: $d/\Lambda = 0.75$, $\Lambda_1/\Lambda = 1.33$, $e \approx 0.83$.

One input parameter for constructing an *MNKLec* structure (with preset D_x, D_y, d, Λ and Λ_1) is the angle between two holes in the first ring, α. In the 6117*cc* structures, α can be varied from 60° (360°/6) to ~51.43° (360°/7).

To characterise the shape of the BMF structure, we use the parameter $\delta = 360°/M - \alpha$. For example, the 6117*cc* structures range in δ from 0° to ~8.57°. In general, the δ of *MNKLcc* circular-core structures ranges from zero to $\delta_{max} = 360°/M - 360°/(M + K)$. The δ range of *MNKLec* elliptical-core structures depends on *e*.

Note that, at $L = 0$, the zero and highest value of the shape parameter δ of the *MNKLcc* structures correspond to symmetric geometries that have, respectively, an *M*-fold and an $(M + K)$-fold rotation axis passing through the fibre axis (the birefringence of the symmetric structures is very low, so these will not be referred to as BMFs). At other δ values, the structures with $N = 1$ and those with $N = 2$ and odd *M* have no rotation axes; there is only a mirror plane, which passes through the fibre axis.

3. Calculation results

The birefringence and dispersion characteristics of the above BMF structures were calculated numerically using the finite element method (FEM), which allows effective modal refractive indices and mode field distributions to be calculated for microstructured fibres with an arbitrary shape and arrangement of air holes. Silica glass was taken as the BMF material, and its refractive index was determined using a Sellmeier equation [23].

The number of holes in the first ring should be at least three. In this study, one BMF type has six holes in the first ring. In the $\delta = 0$ limit, it has a conventional hexagonal structure. The other BMF type has five holes in the first ring. According to preliminary calculations, this configuration ensures a higher birefringence at a given core diameter in comparison with the configuration having six holes in the first ring.

In general, depending on the particular problem, input geometric parameters and conceivable structures, one should perform comparative calculations for BMF structures with different numbers of holes in the first ring in order to find the optimum number, which maximises the birefringence at a preset mode asymmetry.

3.1. Circular-core BMFs

To assess the contribution of the opening to the birefringence of the BMF, we calculated the above circular-core structures at various geometric parameters.

Figure 3a shows the phase birefringence *B* as a function of shape parameter δ for different BMF configurations. For simplicity, we considered structures having one ring of holes ($L = 0$), which had little effect on the birefringence with the d/Λ ratio chosen to be 0.94. Our comparative calculations indicate that a second ring of holes changes the birefringence by less than 5%.

Since the opening width *Z* depends on δ, it is of some interest to know how the phase birefringence *B* varies with *Z*. It can be seen in Fig. 3b that, for $Z \leqslant Z_c \approx 1.5$, the opening depth has little or no effect on the birefringence. This value of Z_c is close to the wavelength the calculations were made for.

In subsequent calculations, the shape parameter δ was taken such that $Z = 2.0$ μm (5.28° for the 6117*cc* and 6125*cc* BMFs and 11.9° for the 5227*cc* and 5243*cc* BMFs). Figure 4a shows the spectral dependences of the phase birefringence *B* and group birefringence *G* for different BMFs. The $B(\lambda)$ data are well fitted by [21]

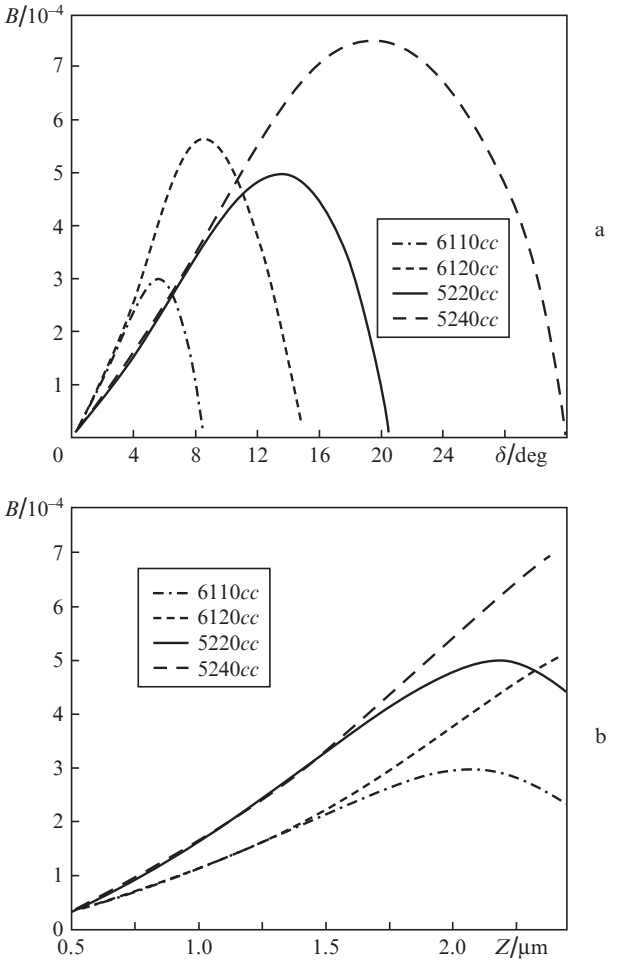

Figure 3. Phase birefringence *B* as a function of (a) shape parameter δ and (b) opening width *Z* for different BMFs: $\lambda = 1.55$ μm, $D = 4.5$ μm, $d/\Lambda = 0.94$.

Table 1.

Parameters	6117*cc*	6125*cc*	5227*cc*	5243*cc*
A (10^{-4})	0.873	1.114	1.422	1.640
γ	2.770	2.798	2.768	2.759
C (10^{-2})	1.867	2.800	3.049	3.841
η	2.761	2.863	2.763	2.829

$$B(\lambda) = A\lambda^{\gamma}, \tag{3}$$

where *A* and γ are parameters (Table 1), and λ is in microns.

The group birefringence *G* was evaluated using the well-known relation [21]

$$G = B - \lambda \frac{dB}{d\lambda}. \tag{4}$$

Substituting (3) into (4) we obtain

$$G(\lambda) = -(\gamma - 1)\, B(\lambda). \tag{5}$$

Figure 4b shows the phase birefringence *B* as a function of core diameter *D* for different BMFs at $\lambda = 1.55$ μm. The $B(D)$ data are well represented by

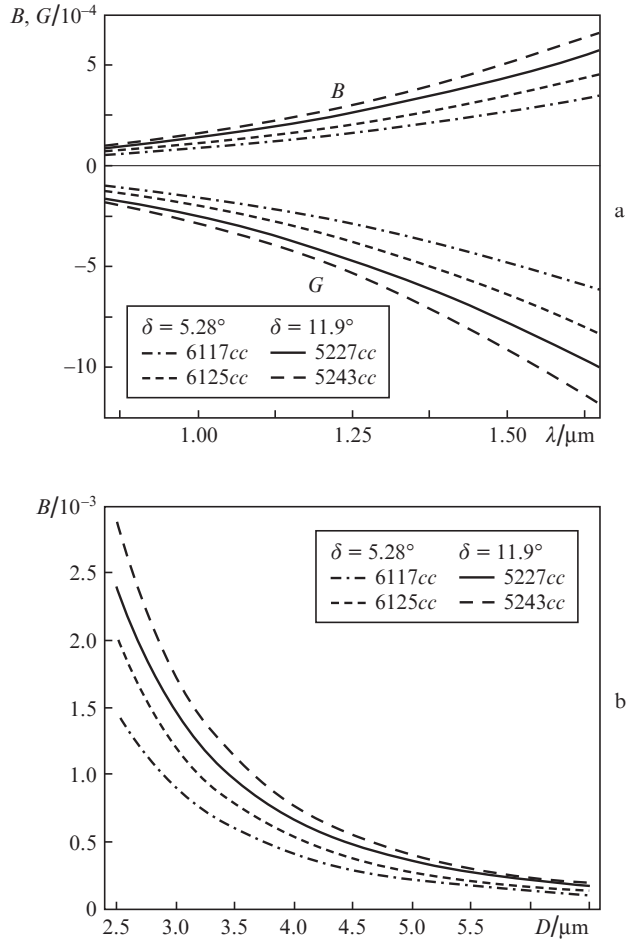

Figure 4. (a) Spectral dependences of the phase birefringence B and group birefringence G for different BMFs at D = 4.5 μm, d/Λ = 0.94 and Z = 2.0 μm. (b) B as a function of core diameter at d/Λ = 0.94 and λ = 1.55 μm.

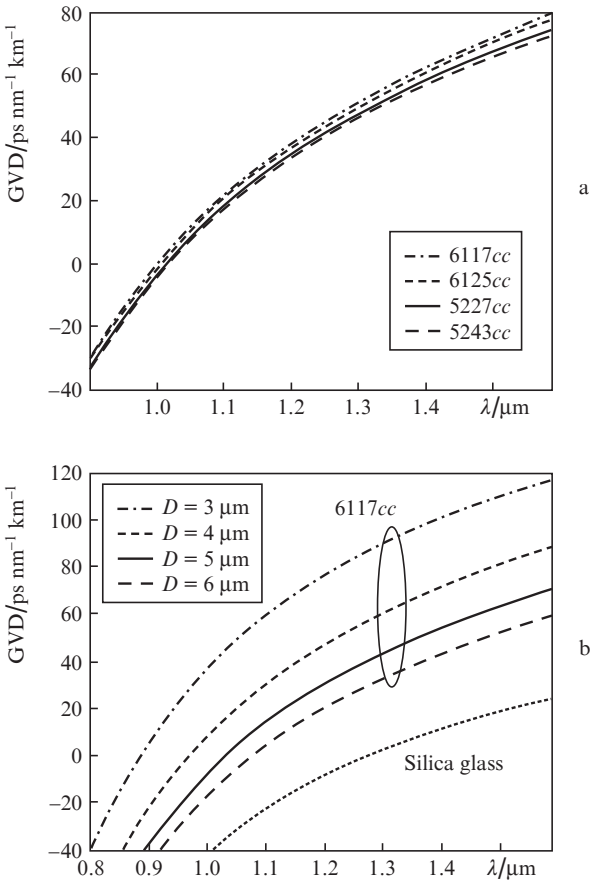

Figure 5. Spectral dependences of group velocity dispersion (GVD) (a) for different BMFs at D = 4.5 μm, d/Λ = 0.94 and Z = 2.0 μm and (b) for 6117*cc* BMFs with d/Λ = 0.94, δ = 5.28° and different core diameters (D). The short-dashed curve in panel b shows the material dispersion of undoped silica glass.

$$B(D) = CD^{-\eta}, \tag{6}$$

where C and η are parameters (Table 1), and D is in microns.

It is worth emphasising that the phase and group birefringences are strong functions of core diameter. For example, BMFs with a 5243*cc* structure and D = 2.5 μm may have $B \sim 3\times10^{-3}$ and $G \sim 5\times10^{-3}$ at 1.55 μm and a low mode asymmetry ($w \approx 0.13$).

For many practical applications, in particular for supercontinuum generation, it is important to know group velocity dispersion (GVD), which is given by [23, p. 18]

$$\mathrm{GVD} \approx -\frac{\lambda}{c}\frac{\mathrm{d}^2 n}{\mathrm{d}\lambda^2}. \tag{7}$$

Figure 5a shows the spectral dependences of group velocity dispersion for different BMFs. The zero dispersion wavelength of the structures ranges from 1.001 to 1.016 μm. Figure 5b presents such data for 6117*cc* BMFs with different core diameters (D). The zero dispersion wavelength here ranges from 0.885 to 1.075 μm. Also shown for comparison is the material dispersion curve of undoped silica glass.

Comparison of Figs 5a and 5b leads us to conclude that the structure of BMFs has a relatively weak effect on the group velocity dispersion in the fibres, whereas the core diameter has a significant effect.

3.2. Elliptical-core BMFs

Elliptical-core BMFs are of interest here for two reasons: first, to accurately calculate the birefringence of real optical fibres, whose core is always somewhat elliptical, and, second, to reduce the mode asymmetry due to the increased hole-to-hole distances in the first ring.

Figure 6 shows the phase birefringence B as a function of shape parameter δ for 6115*ec* and 5223*ec* BMFs with different core ellipticities, e. The birefringence is seen to be higher than that in the circular-core BMFs for $e > 1$ and lower for $e < 1$.

Phase birefringence is commonly defined as

$$B = |n_x - n_y|, \tag{8}$$

where n_x and n_y are the effective refractive indices of two orthogonally polarised modes. Since the structures under consideration have a special direction, that along the opening, and an elliptical core, elongated along or across the opening, we use a different expression for the phase birefringence:

$$B = n_x - n_y. \tag{9}$$

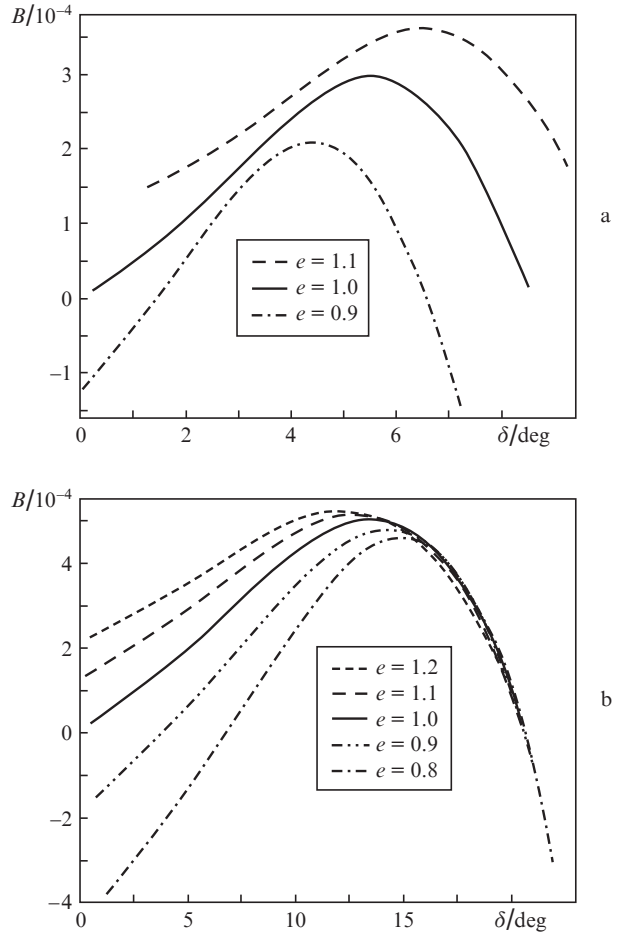

Figure 6. Phase birefringence B as a function of shape parameter δ for (a) 6115*ec* and (b) 5223*ec* BMFs with different core ellipticities (e) at $D_y = 4.5$ μm, $d/\Lambda = 0.94$ and $\lambda = 1.55$ μm.

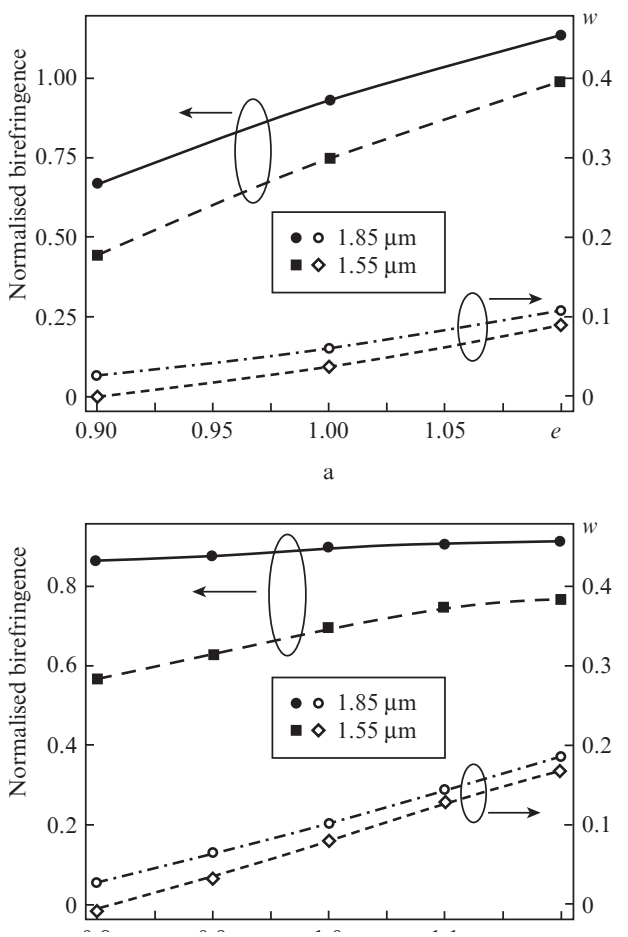

Figure 7. Phase birefringence B and mode asymmetry w as functions of core ellipticity e for (a) 6117*ec* and (b) 5227*ec* BMFs with opening sizes of 1.85 and 1.55 μm; $D_y = 4.5$ μm, $d/\Lambda = 0.94$, $\lambda = 1.55$ μm.

This allows us to retain information about the relationship between the contributions of the opening and elliptical core to the birefringence of the BMF. In particular, for $e < 1$ there are δ ranges where $B < 0$, indicating that the contribution of the core ellipticity to the birefringence of the BMF prevails in such regions.

Figure 7 shows the phase birefringence B and mode asymmetry w as functions of core ellipticity e for 6117*ec* and 5227*ec* BMFs with opening sizes of 1.85 and 1.55 μm. The birefringence is normalised to the maximum birefringence of the circular-core analogues, 2.985×10^{-4} and 5.011×10^{-4} (Fig. 6, data for $e = 1.0$). It can be seen from Fig. 7 that, with increasing opening width, the mode asymmetry parameter of circular-core ($e = 1.0$) 6117*ec* BMFs increases from 0.04 to 0.06 and that of circular-core 5227*ec* BMFs increases from 0.08 to 0.10. It is worth pointing out that the w values obtained indicate that the mode asymmetry in these BMFs is substantially lower than that in the standard BMFs considered by Labonte et al. [21]. In particular, the w values of the mode field profiles calculated by Choi et al. [13] and Lee et al. [22] for BMFs are ~0.45 and ~0.36, respectively, exceeding those of our BMF structures by almost one order of magnitude.

It can be seen from Fig. 7 that, at $Z = 1.55$ μm, the mode field in the 6117*ec* BMF with $e = 0.9$ and in the 5227*ec* BMF with $e = 0.8$ has roughly equal x-axis and y-axis sizes ($w \approx 0$). This is possible because an increased hole-to-hole distance and BMF core ellipticity have different effects on the birefringence and mode asymmetry in the fibre. More precisely, a relatively small opening ensures an increased birefringence, whereas the mode asymmetry remains rather low and can be fully compensated by using a certain core ellipticity, which will slightly reduce the birefringence. Of particular interest in this context is the 5227*ec* BMF with $Z = 1.85$ μm: its birefringence is a weak function of core ellipticity.

Thus, the proposed BMF geometries, with one or two openings between holes in the first ring, allow for high bire-

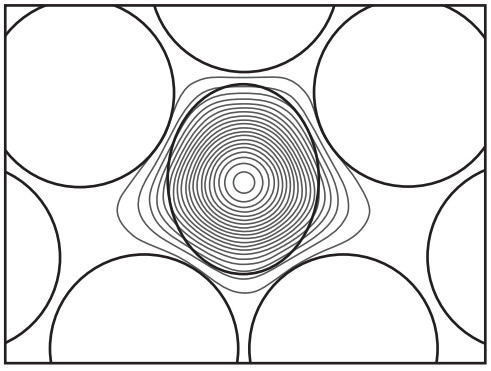

Figure 8. Calculated mode field profile of a 5227*ec* BMF: $Z = 1.55$ μm, $D_y = 4.5$ μm, $e = 0.8$, $d/\Lambda = 0.94$, $\lambda = 1.55$ μm.

fringence at low mode asymmetry. If necessary, the mode asymmetry can be compensated by a slight core ellipticity. This allows one to adjust the relationship between the birefringence and mode asymmetry parameter to a particular problem.

As an illustration, Fig. 8 shows the mode field profile (contours of constant intensity) calculated for a 5227*ec* BMF with two identical openings 1.55 μm in size.

4. Conclusions

We have proposed a novel design of birefringent microstructured fibres. Its key features are that there is one or several concentric rings of holes of the same diameter around an elliptical or circular core and that the holes are the same distance apart except for one or two pairs of holes in the first ring, which are a greater distance apart. Using the finite element method, we have analysed the birefringence and dispersion characteristics of the BMFs. We examined the influence of the core size and shape parameters on the phase and group birefringences of the BMFs and the spectral dependences of group velocity dispersion for different fibre geometries. The results indicate that the proposed BMF design ensures high birefringence ($\sim 5\times10^{-3}$) at a low mode asymmetry. At a certain core ellipticity, the BMF configurations considered may have equal mode field sizes along two orthogonal axes.

We note that, depending on the particular problem, input geometric parameters and conceivable structures, one should perform comparative calculations for BMF structures with different numbers of holes in the first ring in order to find the optimum number, which maximises the birefringence at a preset mode asymmetry.

References

1. Knight J.C., Birks T.A., Russell P.St.J., Atkin D.M. *Opt. Lett.*, **21**, 1547 (1996).
2. Birks T.A., Knight J.C., Russell P.S. *Opt. Lett.*, **22**, 961 (1997).
3. Knight J.C., Skryabin D.V. *Opt. Express*, **15**, 15365 (2007).
4. Knight J.C. *Proc. SPIE–Int. Soc. Opt. Eng.*, **7134**, 713402 (2008).
5. Blondy J.M., Gerome F., Auguste J.L., Restoin C., Humbert G., Roy P., Leproux P., Fevrier S. *Proc. SPIE–Int. Soc. Opt. Eng.*, **7004**, 700404 (2008).
6. Ortigosa-Blanch A., Knight J.C., Wadsworth W.J., Arriaga J., Mangan B.J., Birks T.A., Russell P.St.J. *Opt. Lett.*, **25**, 1325 (2000).
7. Steel M.J., Osgood R.M. Jr. *Opt. Lett.*, **26**, 229 (2001).
8. Hansen T.P., Broeng J., Libori S.E.B., Knudsen E., Bjarklev A., Jensen J.R., Simonsen H. *IEEE Photonics Technol. Lett.*, **13**, 588 (2001).
9. Suzuki K., Kubota H., Kawanishi S., Tanaka M., Fujita M. *Opt. Express*, **9**, 676 (2001).
10. Kim D.-H., Kang J.U. *Opt. Eng.*, **46**, 075003 (2007).
11. Nielsen F.D., Pedersen M.Ø., Qian Y., Andersen T.V., Leick L., Hansen K.P., Pedersen C.F., Thomsen C.L. *CLEO/Europe and IQEC 2007 Conf. Digest* (New York: Opt. Soc. Am., 2007) CJ5_4.
12. Xiong C., Wadsworth W.J. *Opt. Express*, **16**, 2438 (2008).
13. Choi H.-G., Kee C.-S., Sung J.H., Yu T.J., Ko D.-K., Lee J., Park H.Y., Kim J.-E. *Phys. Rev. A*, **77**, 035804 (2008).
14. Zhao C., Dong X. *Asia Commun. Photon. Conf. Exhibit., Techn. Digest (CD)* (New York: Opt. Soc. Am., 2009) TuFF6.
15. Fu H.Y., Wong A.C.L., Childs P.A., Tam H.Y., Liao Y.B., Lu C., Wai P.K.A. *Opt. Express*, **17**, 18501 (2009).
16. Zhang H., Liu B., Wang Z., Luo J., Wang S., Jia C., Ma X. *Optica Applicata*, **40**, 209 (2010).
17. Guan B.-O., Chen D., Zhang Y., Wang H.-J., Tam H.-Y. *IEEE Photonics Technol. Lett.*, **20**, 1980 (2008).
18. Geernaert T., Luyckx G., Voet E., Nasilowski T., Chah K., Becker M., Bartelt H., Urbanczyk W., Wojcik J., De Waele W., Degrieck J., Terryn H., Berghmans F., Thienpont H. *IEEE Photonics Technol. Lett.*, **21**, 6 (2009).
19. Tang J., Chen C., Wang J., Jui P. *Conf. Lasers and Electro-Optics/ Pacific Rim 2007* (New York: Opt. Soc. Am., 2007) MD2_4.
20. Lee H. W., Liu Y., Chiang K.S. *IEEE Photonics Technol. Lett.*, **20**, 132 (2008).
21. Labonte L., Pone E., Skorobogatiy M., Godbout N., Lacroix S., Pagnoux D. *Proc. SPIE–Int. Soc. Opt. Eng.*, **7357**, 73570N (2009).
22. Lee K.J., Hong K.S., Park H.C., Kim B.Y. *Opt. Express*, **16**, 4631 (2008).
23. Agrawal G.P. *Nonlinear Fiber Optics* (San Diego: Academic, 1995; Moscow: Mir, 1996).